ISSN
2395-6992

International Journal of Engineering Research & Science

www.ijoer.com
www.adpublications.org

Volume-9! Issue-9! September, 2023 www.ijoer.com ! info@ijoer.com

Preface

We would like to present, with great pleasure, the inaugural volume-9, Issue-9, September 2023, of a scholarly journal, *International Journal of Engineering Research & Science*. This journal is part of the AD Publications series *in the field of Engineering, Mathematics, Physics, Chemistry and science Research Development*, and is devoted to the gamut of Engineering and Science issues, from theoretical aspects to application-dependent studies and the validation of emerging technologies.

This journal was envisioned and founded to represent the growing needs of Engineering and Science as an emerging and increasingly vital field, now widely recognized as an integral part of scientific and technical investigations. Its mission is to become a voice of the Engineering and Science community, addressing researchers and practitioners in below areas

Chemical Engineering	
Biomolecular Engineering	Materials Engineering
Molecular Engineering	Process Engineering
Corrosion Engineering	
Civil Engineering	
Environmental Engineering	Geotechnical Engineering
Structural Engineering	Mining Engineering
Transport Engineering	Water resources Engineering
Electrical Engineering	
Power System Engineering	Optical Engineering
Mechanical Engineering	
Acoustical Engineering	Manufacturing Engineering
Optomechanical Engineering	Thermal Engineering
Power plant Engineering	Energy Engineering
Sports Engineering	Vehicle Engineering
Software Engineering	
Computer-aided Engineering	Cryptographic Engineering
Teletraffic Engineering	Web Engineering
System Engineering	
Mathematics	
Arithmetic	Algebra
Number theory	Field theory and polynomials
Analysis	Combinatorics
Geometry and topology	Topology
Probability and Statistics	Computational Science
Physical Science	Operational Research
Physics	
Nuclear and particle physics	Atomic, molecular, and optical physics
Condensed matter physics	Astrophysics
Applied Physics	Modern physics
Philosophy	Core theories

Chemistry	
Analytical chemistry	Biochemistry
Inorganic chemistry	Materials chemistry
Neurochemistry	Nuclear chemistry
Organic chemistry	Physical chemistry
Other Engineering Areas	
Aerospace Engineering	Agricultural Engineering
Applied Engineering	Biomedical Engineering
Biological Engineering	Building services Engineering
Energy Engineering	Railway Engineering
Industrial Engineering	Mechatronics Engineering
Management Engineering	Military Engineering
Petroleum Engineering	Nuclear Engineering
Textile Engineering	Nano Engineering
Algorithm and Computational Complexity	Artificial Intelligence
Electronics & Communication Engineering	Image Processing
Information Retrieval	Low Power VLSI Design
Neural Networks	Plastic Engineering

Each article in this issue provides an example of a concrete industrial application or a case study of the presented methodology to amplify the impact of the contribution. We are very thankful to everybody within that community who supported the idea of creating a new Research with IJOER. We are certain that this issue will be followed by many others, reporting new developments in the Engineering and Science field. This issue would not have been possible without the great support of the Reviewer, Editorial Board members and also with our Advisory Board Members, and we would like to express our sincere thanks to all of them. We would also like to express our gratitude to the editorial staff of AD Publications, who supported us at every stage of the project. It is our hope that this fine collection of articles will be a valuable resource for *IJOER* readers and will stimulate further research into the vibrant area of Engineering and Science Research.

Mukesh Arora

(Chief Editor)

Board Members

Dr. M. Varatha Vijayan

Annauniversity Rank Holder, Commissioned Officer Indian Navy, Ncc Navy Officer (Ex-Serviceman Navy), Best Researcher Awardee, Best Publication Awardee, Tamilnadu Best Innovation & Social Service Awardee From Lions Club.

Dr. Mohamed Abdel Fatah Ashabrawy Moustafa

PhD. in Computer Science - Faculty of Science - Suez Canal University University, 2010, Egypt.

Assistant Professor Computer Science, Prince Sattam bin AbdulAziz University ALkharj, KSA.

Prof.S.Balamurugan

Dr S. Balamurugan is the Head of Research and Development, Quants IS & CS, India. He has authored/co-authored 35 books, 200+ publications in various international journals and conferences and 6 patents to his credit. He was awarded with Three Post-Doctoral Degrees - Doctor of Science (D.Sc.) degree and Two Doctor of Letters (D.Litt) degrees for his significant contribution to research and development in Engineering.

Dr. Mahdi Hosseini

Dr. Mahdi did his Pre-University (12^{th}) in Mathematical Science. Later he received his Bachelor of Engineering with Distinction in Civil Engineering and later he Received both M.Tech. and Ph.D. Degree in Structural Engineering with Grade "A" First Class with Distinction.

Dr. Anil Lamba

Practice Head – Cyber Security, EXL Services Inc., New Jersey USA.

Dr. Anil Lamba is a researcher, an innovator, and an influencer with proven success in spearheading Strategic Information Security Initiatives and Large-scale IT Infrastructure projects across industry verticals. He has helped bring about a profound shift in cybersecurity defense. Throughout his career, he has parlayed his extensive background in security and a deep knowledge to help organizations build and implement strategic cybersecurity solutions. His published researches and conference papers has led to many thought provoking examples for augmenting better security.

Dr. Ali İhsan KAYA

Currently working as Associate Professor in Mehmet Akif Ersoy University, Turkey.

Research Area: Civil Engineering - Building Material - Insulation Materials Applications, Chemistry - Physical Chemistry – Composites.

Dr. Parsa Heydarpour

Ph.D. in Structural Engineering from George Washington University (Jan 2018), GPA=4.00.

Dr. Heba Mahmoud Mohamed Afify

Ph.D degree of philosophy in Biomedical Engineering, Cairo University, Egypt worked as Assistant Professor at MTI University.

Dr. Aurora Angela Pisano

Ph.D. in Civil Engineering, Currently Serving as Associate Professor of Solid and Structural Mechanics (scientific discipline area nationally denoted as ICAR/08"–"Scienza delle Costruzioni"), University Mediterranea of Reggio Calabria, Italy.

Dr. Faizullah Mahar

Associate Professor in Department of Electrical Engineering, Balochistan University Engineering & Technology Khuzdar. He is PhD (Electronic Engineering) from IQRA University, Defense View, Karachi, Pakistan.

Prof. Viviane Barrozo da Silva

Graduated in Physics from the Federal University of Paraná (1997), graduated in Electrical Engineering from the Federal University of Rio Grande do Sul - UFRGS (2008), and master's degree in Physics from the Federal University of Rio Grande do Sul (2001).

Dr. S. Kannadhasan

Ph.D (Smart Antennas), M.E (Communication Systems), M.B.A (Human Resources).

Dr. Christo Ananth

Ph.D. Co-operative Networks, M.E. Applied Electronics, B.E Electronics & Communication Engineering Working as Associate Professor, Lecturer and Faculty Advisor/ Department of Electronics & Communication Engineering in Francis Xavier Engineering College, Tirunelveli.

Dr. S.R.Boselin Prabhu

Ph.D, Wireless Sensor Networks, M.E. Network Engineering, Excellent Professional Achievement Award Winner from Society of Professional Engineers Biography Included in Marquis Who's Who in the World (Academic Year 2015 and 2016). Currently Serving as Assistant Professor in the department of ECE in SVS College of Engineering, Coimbatore.

Dr. PAUL P MATHAI

Dr. Paul P Mathai received his Bachelor's degree in Computer Science and Engineering from University of Madras, India. Then he obtained his Master's degree in Computer and Information Technology from Manonmanium Sundaranar University, India. In 2018, he received his Doctor of Philosophy in Computer Science and Engineering from Noorul Islam Centre for Higher Education, Kanyakumari, India.

Dr. M. Ramesh Kumar

Ph.D (Computer Science and Engineering), M.E (Computer Science and Engineering).

Currently working as Associate Professor in VSB College of Engineering Technical Campus, Coimbatore.

Dr. Maheshwar Shrestha

Postdoctoral Research Fellow in DEPT. OF ELE ENGG & COMP SCI, SDSU, Brookings, SD Ph.D, M.Sc. in Electrical Engineering from SOUTH DAKOTA STATE UNIVERSITY, Brookings, SD.

Dr. D. Amaranatha Reddy

Ph.D. (Postdocteral Fellow, Pusan National University, South Korea), M.Sc., B.Sc. : Physics.

Dr. Dibya Prakash Rai

Post Doctoral Fellow (PDF), M.Sc., B.Sc., Working as Assistant Professor in Department of Physics in Pachhuncga University College, Mizoram, India.

Dr. Pankaj Kumar Pal

Ph.D R/S, ECE Deptt., IIT-Roorkee.

Dr. P. Thangam

PhD in Information & Communication Engineering, ME (CSE), BE (Computer Hardware & Software), currently serving as Associate Professor in the Department of Computer Science and Engineering of Coimbatore Institute of Engineering and Technology.

Dr. Pradeep K. Sharma

PhD., M.Phil, M.Sc, B.Sc, in Physics, MBA in System Management, Presently working as Provost and Associate Professor & Head of Department for Physics in University of Engineering & Management, Jaipur.

Dr. R. Devi Priya

Ph.D (CSE), Anna University Chennai in 2013, M.E, B.E (CSE) from Kongu Engineering College, currently working in the Department of Computer Science and Engineering in Kongu Engineering College, Tamil Nadu, India.

Dr. Sandeep

Post-doctoral fellow, Principal Investigator, Young Scientist Scheme Project (DST-SERB), Department of Physics, Mizoram University, Aizawl Mizoram, India- 796001.

Dr. Roberto Volpe

Faculty of Engineering and Architecture, Università degli Studi di Enna "Kore", Cittadella Universitaria, 94100 – Enna (IT).

Dr. S. Kannadhasan

Ph.D (Smart Antennas), M.E (Communication Systems), M.B.A (Human Resources).

Research Area: Engineering Physics, Electromagnetic Field Theory, Electronic Material and Processes, Wireless Communications.

Mr. Amit Kumar

Amit Kumar is associated as a Researcher with the Department of Computer Science, College of Information Science and Technology, Nanjing Forestry University, Nanjing, China since 2009. He is working as a State Representative (HP), Spoken Tutorial Project, IIT Bombay promoting and integrating ICT in Literacy through Free and Open Source Software under National Mission on Education through ICT (NMEICT) of MHRD, Govt. of India; in the state of Himachal Pradesh, India.

Mr. Tanvir Singh

Tanvir Singh is acting as Outreach Officer (Punjab and J&K) for MHRD Govt. of India Project: Spoken Tutorial - IIT Bombay fostering IT Literacy through Open Source Technology under National Mission on Education through ICT (NMEICT). He is also acting as Research Associate since 2010 with Nanjing Forestry University, Nanjing, Jiangsu, China in the field of Social and Environmental Sustainability.

Mr. Abilash

MTech in VLSI, BTech in Electronics & Telecommunication engineering through A.M.I.E.T.E from Central Electronics Engineering Research Institute (C.E.E.R.I) Pilani, Industrial Electronics from ATI-EPI Hyderabad, IEEE course in Mechatronics, CSHAM from Birla Institute Of Professional Studies.

Mr. Varun Shukla

M.Tech in ECE from RGPV (Awarded with silver Medal By President of India), Assistant Professor, Dept. of ECE, PSIT, Kanpur.

Mr. Shrikant Harle

Presently working as a Assistant Professor in Civil Engineering field of Prof. Ram Meghe College of Engineering and Management, Amravati. He was Senior Design Engineer (Larsen & Toubro Limited, India).

Zairi Ismael Rizman

Senior Lecturer, Faculty of Electrical Engineering, Universiti Teknologi MARA (UiTM) (Terengganu) Malaysia Master (Science) in Microelectronics (2005), Universiti Kebangsaan Malaysia (UKM), Malaysia. Bachelor (Hons.) and Diploma in Electrical Engineering (Communication) (2002), UiTM Shah Alam, Malaysia.

Mr. Ronak

Qualification: M.Tech. in Mechanical Engineering (CAD/CAM), B.E.

Presently working as a Assistant Professor in Mechanical Engineering in ITM Vocational University, Vadodara. Mr. Ronak also worked as Design Engineer at Finstern Engineering Private Limited, Makarpura, Vadodara.

Table of Contents

Volume-9, Issue-9, September 2023

Factorial Analysis of Soil pH as a Function of Its Moisture Content and Distance from Flare Point

C. I. Nwoye[1*], C. N. Nwambu[2], C. C. Emekwisia[3]

Chemical Systems Research and Empirical Model Laboratory
Department of Metallurgical and Materials Engineering, Nnamdi Azikiwe University, Awka, Nigeria
*Corresponding Author

Received: 04 September 2023/ Revised: 16 September 2023/ Accepted: 21 September 2023/ Published: 30-09-2023

Abstract— *This paper presents a derived model which predicts the soil pH based on its soil moisture content and distance from flare point. The response coefficient of the soil pH to the distance from flare point and soil moisture content was evaluated to ascertain the viability and reliability of the highlighted dependence. Results of series of evaluations carried out indicate that the correlations between soil pH and distance from flare point & soil moisture content as evaluated from the actual and model-predicted results were all > 0.88. Standard errors incurred in obtaining results of soil pH based on distance from flare point & moisture content were 0.08 and 0.07 & 0.076 and 0.06%, as obtained from actual and model-predicted results respectively. The validity of the model;* $\xi = -0.0496\beta^2 - 1.5 \times 10^{-7}\vartheta + 0.7122\beta + 0.0003\vartheta + 2.5408$ *was rooted on the insignificant maximum deviation of model-predicted values of soil pH from the corresponding actual values which was less than 1.1%. This translated into over 98.9% operational confidence level for the derived model as well as over 0.98 response coefficient of soil pH to the combined operational influence of distance from flare point and soil moisture content.*

Keywords— Analysis, soil pH, distance from flare site, and soil moisture content.

I. INTRODUCTION

Investigations [1] carried out to measure physicochemical parameters in flare sites have shown that pH of soil and rain-water samples are acidic in nature if collected at varied distances of 20, 50 and 100 m from flare points. This implies presence of acid rains and acid soils around the flare locations. The results of the investigation also reveal that soils and rain water are contaminated by heavy metals such as Cr, Cd, As, Pb, Zn, Fe. The research findings further show that higher concentration of air quality parameters (such as SO_2, NO_2, H_2S, CO, VOC, SPM etc.) exists at least distances near the flare point and lower values at distances farther away from flare point.

Research [2] has shown that apart from the fact that gas flaring activities in the Niger-Delta region pose very serious environmental implications on the host communities, it is an economic wastage of natural resource to Nigeria. For example, acid compounds are formed when NOx and SO_2 gases contained in gas flares reacts with water. This has placed gas flaring as being responsible for the acid rain syndrome often experienced in the Niger Delta region.

It has been revealed [1] that high pollution loads are imposed on gas flaring environments arising from increased pH of soil and acid rain concentrations (due to gas emissions), abnormal air temperature (due to flare radiation), heavy metal concentration and poor air quality due to flare emissions (particularly CO, NO_2, SO_2, smoke and particulate matter contents). This has impacted negatively on human habitats and as a result, no meaningful human activity can take place at gas flaring locations within radial distances < 2 km away from flare point.

Some undermining effects of gas flaring on locations and its inhabitants has been reported [3] to include poor soil fertility (due to soil pH, heavy metals and toxics pollution), health hazards (such as skin problems, cancer, reproductive health problems, respiratory disorders etc.), climate change (bringing about flooding).

Some research works [4], [5],[6] and [7] have corroborated earlier finding [3] that gas flaring is also the major cause low agricultural productivity, depleted success in fishing and hunting due to incessant acid rain. This causes impoverishment in the Niger Delta. The poor agricultural activities were observed [4] to be as a result of release of some substances which alters the

surface and ground water quality, aggregate nutrient deficiencies in soils, or accelerate the soiling, weathering or corrosion of engineering and cultural materials. Furthermore, visible changes exist in soil characteristics close to a flare site.

Factors such as distance of sample from source of flare, duration of flare and height of flare stack have been observed [1] to absolutely affect the distribution (or spread) of soils physicochemical parameters in a gas flaring environments. These research outputs are in line with earlier report [8] where soil pH values changed from acidic to near neutral as soil samples were collected some distances away from flare point.

Results [9] of insitu and laboratory tests indicate that gas flare effect pH, temperature and moisture content of soils negatively. The results reveal that pH showed the least value (most acidic) of 5.12 at depth of 5cm and distance of 200m away from the flare. The soil temperature at 200m and 5cm depth, recorded the highest value (39.7^0C) and the least value (27^0C) at 35000m (control site) away. The least value for moisture content (5.83%) was recorded at 200m and the highest (15.38%) at the control site.

This work attempts to derive a model which will predict the soil pH based on its soil moisture content and distance from flare point.

TABLE 1
VARIATION OF SOIL PH WITH ITS MOISTURE CONTENT AND DISTANCE FROM FLARE POINT [10]

(ϑ) (m)	(β)	(ξ)
200	5.83	5.09
500	8.13	5.12
750	7.68	5.25
1000	7.11	5.27
1200	6.58	5.18
1500	6.35	5.12

II. MATERIAL AND METHOD

2.1 Model formulation

Computational analysis (using C-NIKBRAN [11]) of results in Table 1 indicates that

$$\xi - K = -Ъ\beta^2 - S\vartheta^2 + N\beta + C\vartheta \quad (1)$$

Introducing the values of Ъ and K into equation (1) reduces it to

$$\xi - 2.5408 = - 0.0496\ \beta^2 - 1.5\ x10^{-7}\vartheta + 0.7122\beta + 0.0003\vartheta \quad (2)$$

$$\xi = - 0.0496\ \beta^2 - 1.5\ x10^{-7}\vartheta + 0.7122\beta + 0.0003\vartheta + 2.5408 \quad (3)$$

Where

(ϑ) = Distance from flare point (m)

(ξ) = Soil pH at distance ϑ from flare point (%)

(β) = Soil moisture content at distance ɣ where the soil pH was evaluated

K , Ъ, S, N and C are equalizing constants; 2.5408, 0.0496, 1.5 $X10^{-7}$, 0.7122 and 0.0003 respectively.

III. BOUNDARY AND INITIAL CONDITIONS

The ranges of distance from flare site, soil pH and soil moisture content are 200 -1500m, 5.09- 5.27, and 5.83 – 8.13(%) respectively.

IV. RESULTS AND DISCUSSION

4.1 Model validation

Validation of the model was carried out by statistical, graphical and deviational methods.

TABLE 2
VARIATION OF $\xi - 2.5408$ with $- 0.0496\beta^2 - 1.5 \times 10^{-7}\vartheta + 0.7122\beta + 0.0003\vartheta$

$\xi - 2.5408$	$- 0.0496\beta^2 - 1.5 \times 10^{-7}\vartheta + 0.7122\beta + 0.0003\vartheta$
2.5492	2.5203
2.5792	2.6243
2.7092	2.6848
2.7292	2.7063
2.6392	2.6794
2.5792	2.635

The derived model was rooted in equation (2). Equation (2) agrees with Table 2 following the values of $\xi - 2.5408$ and $- 0.0496\beta^2 - 1.5 \times 10^{-7}\vartheta + 0.7122\beta + 0.0003\vartheta$ evaluated from Table 1.

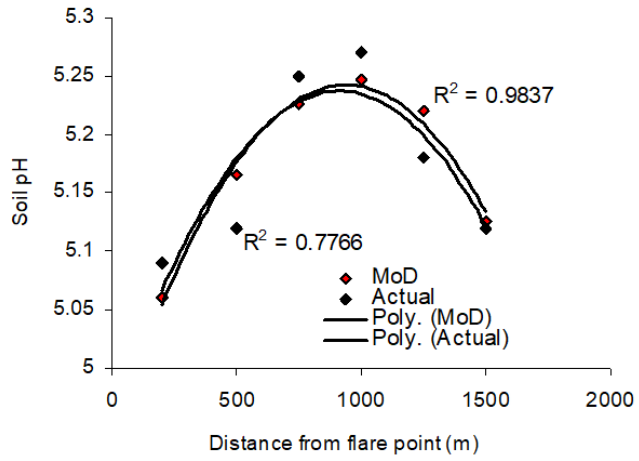

FIGURE 1: Comparison of the correlations of the actual and model-predicted soil pHs (relative to distance from flare point)

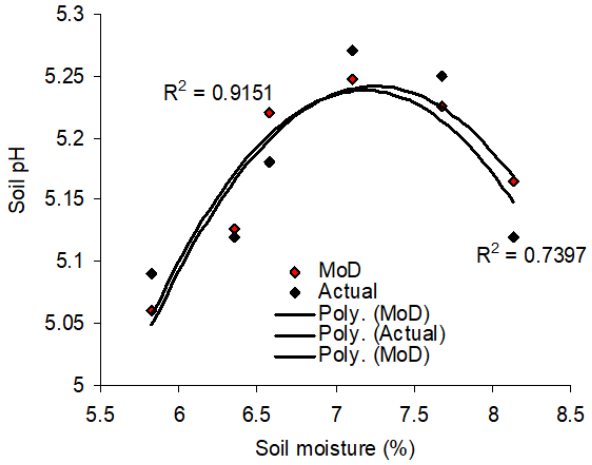

FIGURE 2: Comparison of the correlations of the actual and model-predicted soil pHs (relative to soil moisture)

4.2 Statistical Analysis

4.2.1 Standard Error (STEYX)

The standard errors incurred in predicting the soil pH for each value of the distance from flare point & soil moisture content considered as obtained from actual and derived model were 0.08 and 0.07 & 0.076 and 0.06 % respectively. The standard error was evaluated using Microsoft Excel version 2003.

4.2.2 Correlation (CORREL)

Comparison of the correlations of the actual and model-predicted soil pHs relative to both distance from flare point and soil moisture content were evaluated (using Microsoft Excel Version 2003) from results of the actual and derived model. These evaluations were based on the coefficients of determination R^2 shown in Figs. 1 and 2.

$$R = \sqrt{R^2} \tag{4}$$

These correlations are 0.9918 & 0.8812 and 0.9566 & 0.8601 respectively. These evaluated results indicate that the derived model predictions are significantly reliable and hence valid considering its proximate agreement with results from actual experiment.

4.3 Graphical Analysis

Analysis of Figs 3 and 4 shows close alignment of the curves of model-predicted soil pH (relative to distance from flare point and soil moisture content) and those from the actual results.

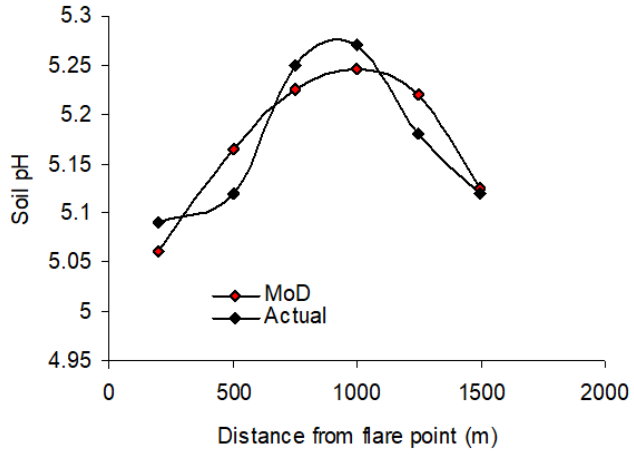

FIGURE 3: Comparison of the soil pHs (relative to distance from flare point) as obtained from actual and model-predicted results

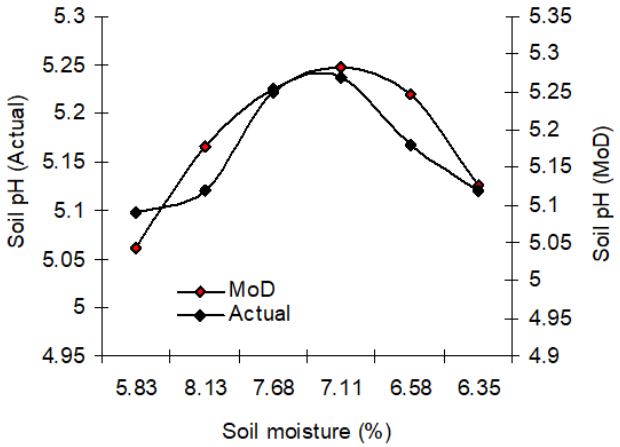

FIGURE 4: Comparison of the soil pHs (relative to soil moisture content) as obtained from actual and model-predicted results

Figs.3-4 strongly indicates that the degree of alignment of curves is indicative of the proximate agreement between both actual and model-predicted values of soil pH. This also indicates that the derived model is valid, reliable and of very high operation confidence.

4.4 Deviational Analysis

Analysis of soil pH as obtained from actual and derived model show deviation of model-predicted values from those of the actual. This is believed to be due to the fact that some considered assumptions and experiment-oriented conditions which prevailed during the actual field work were not considered during the model formulation. This necessitated the introduction of correction factor, to bring the model-predicted values to those of the actual.

Deviation (Dv) (%) of the model-predicted soil pH from that of the actual is given by

$$Dv = \frac{\xi p - \xi a}{\xi a} \times 100 \quad (5)$$

Where

ξp = Model-predicted soil pH

ξa = Soil pH evaluated from actual results

Table 3 shows that the least and highest deviations of model-predicted results (from actual results) are – 0.43 and + 1.09%. These deviations correspond to model-predicted soil pHs: 5.2471 & 5.1758; distance from flare points: 1000 & 1500m, and soil moisture content: 7.11 & 6.35% respectively.

TABLE 3
ACTUAL SOIL PH AND CORRESPONDING PERCENT DEVIATION OF MODEL-PREDICTED RESULTS

(ξ)	Dv (%)	Cf(%)
5.09	-0.57	0.57
5.12	0.88	-0.88
5.25	-0.46	0.46
5.27	-0.43	0.43
5.18	0.78	-0.78
5.12	1.09	-1.09

Correction factor (Cr) is the negative of the deviation i.e

$$Cr = - Dv \quad (6)$$

Therefore

$$Cr = -100\left\{\frac{\xi p - \xi a}{\xi a}\right\} \times 100 \quad (7)$$

Introduction of the corresponding values of Cf from equation (7) into the model gives exactly the corresponding actual values.

Equations (6) and (7) show that correction factor is the negative of the deviation. It is strongly believed that the correction factor takes care of the assumptions made and experimental condition prevailing during the field works which were not considered during the model formulation.

Table 3 also revealed that the least and highest deviations of model-predicted results (from actual results) are + 0.43 and - 1.09%. These deviations also correspond to model-predicted soil pHs: 5.2471 & 5.1758; distance from flare points: 1000 & 1500m, and soil moisture content: 7.11 & 6.35% respectively.

The deviation of model predicted results from that of the actual is just the magnitude of the value. The associated sign preceding the value signifies that the deviation is deficit (negative sign) or surplus (positive sign).

V. CONCLUSION

Following derivation of a model for prediction of the soil pH based on its soil moisture content and distance from flare point, the correlations between soil pH and distance from flare point & soil moisture content as evaluated from the actual and model-predicted results were all > 0.88. Standard errors incurred in obtaining results of soil pH based on distance from flare point & moisture content were 0.08 and 0.07 & 0.076 and 0.06%, as obtained from actual and model-predicted results respectively. The validity of the model; $\xi = -0.0496\,\beta^2 - 1.5 \times 10^{-7}\vartheta + 0.7122\beta + 0.0003\vartheta + 2.5408$ was rooted on the insignificant maximum deviation of model-predicted values of soil pH from the corresponding actual values which was less than 1.1%. This translated into over 98.9% operational confidence level for the derived model as well as over 0.98 response coefficient of soil pH to the combined operational influence of distance from flare point and soil moisture content.

REFERENCES

[1] Uyigue L, and Enujekwu F. M.(2017). Physicochemical Analysis of Gas Flaring Impact on the Environment of Host Communities in the Niger-delta. Journal of Environment Pollution and Human Health, 5(1): 22-29. doi: 10.12691/jephh-5-1-4.

[2] Sonibare, J. A. and Akeredolu, F. A. (2004). A review of the usefulness of gas flares in air pollution control. Management of environmental quality: An international journal, 15(6): 574-583.

[3] Ajugwo, A. O. (2013). Negative effects of gas flaring: The Nigerian Experience. Journal of Environmental Pollution and Human Health. 1(1), 6-8.

[4] Alakpodia. I.J, Soil characteristics under gas flare in the Niger Delta, Southern Nigeria. Geo-studies forum.1 (1 and 2): 2000, 1-10.

[5] Dauda. O.D, Socio-economic and Environmental problems associated with oil spillage in the Niger Delta,(M.Sc. Thesis), 2001, School of Environmental sciences, Imo State University. Owerri, Nigeria

[6] Odjugo. P.A.O, Health Safety and Environment: Challenges of the Environmental Health. Officers in the present democratic dispensation. Paper presented at the 3rd Delta State Triennial delegates conference/NEC meeting held at Asaba, Delta State, Nigeria, 13- 15 June, 2002.

[7] Akudo, E.O, Fezighe, I.O and Ossai-Abeh, E (2012). The Impact of Distance on Soil Temperature and Moisture Content in a Gas Flare Site., African Journal of Physical Sciences, 5(2)

[8] Ubani, E. C. and Onyejekwe, I. M. (2013). Environmental impact analyses of gas flaring in the Niger-Delta region of Nigeria. American Journal of Scientific and Industrial Research.4(2), 246-252.

[9] Ernest A. Orji, Boniface C.E. Egboka , Asheshe U.S and Dio B.A(2015). Influence of Gas Flaring on some physical Properties of Soils in Kwale, Delta State. IOSR Journal of Environmental Science, Toxicology and Food Technology (IOSR-JESTFT) Ver. I, 9(8):52-57

[10] E. A. Orji, B. C. E. Egboka, U. S. Asheshe and B. A. Dio (2015). Influence of Gas Flaring on Some Physical Properties of Soils in Kwale, Delta State. IOSR Journal of Environmental Science, Toxicology and Food Technology, 9(8) 52-57.

[11] Nwoye, C. I. (2008). Data Analytical Memory; C-NIKBRAN.

The Development of Cellulose Nanocrystals Reinforced with Carboxylmethyl Cellulose/Gelatin for Biodegradable Packaging

E. C. Nwanna[1*], L. C. Orakwe[2], P. C. Eze[3], C.P. Nwachukwu[4], A. E. Ekpo[5], J. I. Maduegbuna[6]

[1,2,4,5,6]Department of Agricultural and Bioresources Engineering, Nnamdi Azikiwe University, P. M. B 5025, Awka, Nigeria.
[3]Department of Agricultural & Bioresources Engineering, Enugu State University of Science & Technology Enugu State, Nigeria.
*Corresponding Author

Received: 01 September 2023/ Revised: 13 September 2023/ Accepted: 20 September 2023/ Published: 30-09-2023

Abstract— *It has significant potential to strengthen carboxymethyl cellulose/gelatin nanocomposite with cellulose nanocrystals from plantain stems for the production of bioplastics. Alkaline pretreatment and acid hydrolysis were used to extract cellulose nanocrystals from plantain stem. Films made of carboxymethyl cellulose and gelatin were strengthened using cellulose nanocrystals made from plantain stem fiber. SEM, thermogravimetric analysis (TGA), and water vapour permeability (WVP) were used to characterize the synthetic bioplastic's physical properties. The environmental deterioration of the bioplastic samples was observed over time at regular intervals in soil that was taken from a waste landfill. The results showed that the water vapour permeability of the investigated films was decreased by the addition of CNC from 2.45 x 10^{-6}g/m x h x Pa to 1.73 x 10^{-6}g/m x h x Pa. Additionally, it was discovered that unreinforced films degraded by 0.2% after 35 days, whereas 5wt% and 10wt% CNC reinforced films lost weight as a result of biodegradation by 0.1% and 0.18%, respectively. Overall, the interconnected carboxymethyl cellulose/gelatin bolstered CNC nanocomposite film for making plastics increased the heat and water vapour permeability of the packaging film, which offers the chances of their packaging application*.

Keywords— Plantain stem, packaging material, carboxymethyl cellulose, gelatin, and bioplastics.

I. INTRODUCTION

Hydrocarbon packaging materials currently pose a serious hazard to the environment as they are unable to decompose naturally and the scarcity of petroleum feedstock (Goh et al., 2016). Toxic waste production should be decreased by employing environmentally friendly and renewable methods. About 300 million metric tonnes of synthetic polymer will be discharged into the environment in 2018, with half of that quantity being released without being sorted, based on the assessment conducted by (Ogunola et al., 2018). Recycling plastic is not always easy because end products made from these wastes might not be suitable for use in post-consumer goods and because mixed plastic pollutants might cause problems. The demand for bioplastic as an alternative to traditional plastics has risen exponentially because to its non-toxicity, biocompatibility, renewability, and biodegradability features (Mostafa et al., 2020). Biobased plastics can be degraded by microbial processes using a variety of raw materials (proteins and polysaccharides), largely generated from plants (cellulose-based plastics and starch-derived plastics), as well as algae and bacteria such polyhydroxyalkanoates (PHAs) and polylactic acid (PLA). The amount of the plastic material is significant because it has the potential to be dangerous toward each human, communities, and the entire ecosystem (Gerritse et al., 2020; Mateos-Cárdenas et al., 2020). As a result, an increase in waste volume was caused by an unrestrained population growth and an excessive use of non-renewable resources. Only a few methods exist at the moment for partially eradicating harmful wastes, such as landfills and ocean discharges of an assortment of materials, some of which can decompose in a predetermined amount of time while other garbage cannot decompose for hundreds of years. The bio bags, on the other hand, were expected to differ from conventional plastic bags only little (Fernández-Braa et al., 2019). All these issues with conventional plastic have been addressed by the introduction of biopolymers, which maintains remarkable distinctive qualities and is more reliable today. It could be among the best solutions to fill the void left by the widespread prohibition of regular plastic. Biodegradable plastics are obviously manufactured from renewable biomass resources including vegetable and

fruit garbage, biopolymers, and microorganisms (Yaradoddi et al., 2019). Biodegradable polymers can be broken down into smaller bits through aerobic or anaerobic biological processes. The procedure is frequently explained in terms of the kinds of bioplastics employed, such as starch, cellulose, and materials made of biopolymers.

As appealing alternatives to synthetic-based plastic packaging materials, biopolymers derived from a variety of natural resources, such as cellulose, chitosan, starch, soy, zein, and other proteins from plant and animal sources, have been considered (Tang et al., 2012). Due to their advantageous characteristics, these natural polymers packaging materials increase the quality and shelf life of the packed commodities (Han and Gennadios, 2005). One of the components that is utilized the most frequently in the production of bioplastics is carboxymethyl cellulose (CMC). It is a translucent, non-toxic synthetic polymer with a top standard of biocompatibility as well as biodegradability. It has excellent film-forming capabilities, is highly polar, highly soluble in water, and causes a number of beneficial associations with hydroxyl groups (Naduparambath et al., 2018). The prospect of interaction and blending with other polar polymers is thus suggested (Ismaiel et al., 2018). Gelatin is used to make biodegradable films, but it is also a soluble, pleasant, and renewable material. It is an animal protein that is made from collagen through acid hydrolysis or alkaline hydrolysis.

It is widely used in the food and pharmaceutical industries (Alves et al., 2015). Gelatin is employed in packaging for a number of reasons, including its accessibility, cost, versatility, as well as protective action towards gas flow (Ramos et al., 2016). Furthermore, cellulose nanocrystal is among the most studied bio-based reinforcements (CNC). According to Moon et al., (2011), cellulose nanocrystal particles typically have a crystallinity index that fluctuates around 54 to 88%, a width of 20 to 50 nm, and fiber lengths of 100 to 250 nm. The CNC is created by acid or enzymatic hydrolysis of cellulose fibers. They are used as replacements in polymeric composites because of their unique properties, such as high modulus, the ability to generate a highly porous structure, huge surface area, biodegradability, as well as environmental benefits (Mariano et al., 2016; Ferreira et al., 2017). It is possible to separate cellulose nanocrystals from a variety of natural sources of cellulose. The most accessible and prolific of these sources is plant biomass. They therefore have the greatest potential for mass producing CNCs. Shape, size, and degree of polymerization are a few properties of nanocellulose that rely not only on the isolation techniques used in addition to origin through which they were derived (Habibi et al., 2010). One of the cellulose-containing natural fibers is found in the plantain stem (Musa paradisiaca). It is a substantial staple food in Nigeria and other humid tropical countries in Africa, America, and the Caribbean (Ketiku, 1973; Baiyeri and Unadike, 2007). It is a natural fiber product whose potential has not yet been fully realized. Thus, processing plantains can boost product variety, market price, and usage whilst still positively contributing. The use of CNC to improve the properties of popular film-forming mixtures like gelatin/CMC is not well supported by research. This approach is based on the idea that a bothersome plantain stem fiber can be given value in order to assist speedy deconstruction and packaging of meals for on-the-go eating. The results of the study should provide new applications for plantain stems and contribute to addressing pressing environmental issues associated with the usage of petroleum-based and non-biodegradable plastics in food packaging, especially for goods that need to be consumed on the go.

II. MATERIALS AND METHODS

2.1 Materials

The Onitsha Bridge-head Chemical Market in Anambra State, Nigeria, provided the ingredients. The analytical grades of gelatin (bloom strength 185), glycerol (98%), sulphuric acid (99%), sodium hydroxide, sodium chlorite, acetic acid (98%), benzene (99%), ethanol (99%), calcium chloride (96%) and potassium sulphate (99%). The analytical grades of carboxylmethyl cellulose (molecular weight, 115 000 g/mol; degree of polymerization, 1700-1800). The plantain stem fiber came from Okeanyanwu's plantation in Awka Town, Awka South Local Government Area, Anambra State, Nigeria.

2.2 Extraction of cellulose pulp

Cellulose was extracted from the plantain stem fibre (PSF) using a similar technique by EL Miri et al., (2015), with a little alteration. Carefully selected, cleaned, and dried fiber was used. The fiber was ground into a powder, sieved to a thickness of 150 m, and diced to a length of about 10 mm before being cooked in a sodium hydroxide solution. For this treatment, 17.5% (w/v) sodium hydroxide was employed for 1 hour at 80 °C. The generated fibers were thoroughly cleaned with distilled water before being dried in an oven at 100 °C to a constant weight. A previously documented bleaching procedure involved bleaching 1 g of dry fiber for 1 h at 75 °C using 0.6 g sodium chlorite, 0.5 ml acetic acid, and 65 ml distilled water (EL Miri et al., 2015). Due to the continuous injection of extra bleaching solution at 1-hour intervals, the fibers had gone white after 4 hours. After properly cleaning them with distilled water, the fibers were left to air dry to their ultimate weight.

2.3 Plantain stem cellulose nanocrystal (CNC) preparation

The CNC was produced by controlled sulphuric acid hydrolysis using 8.75 mL of 64 weight percent sulphuric acid (H_2SO_4) and 1g of dried cellulose pulp. The mixture was vigorously stirred at 45°C for 30 minutes, according to earlier findings (Csiszár and Nagy, 2017; Kargarzadeh et al., 2017). When the timer went off, ten rounds of ice-cold deionized water were used to stop the reaction. The cold solution was centrifuged for 10 minutes at 8500 rpm, and the liquid supernatant was decanted. The solid was centrifuged and diluted constantly until it became murky. To achieve a pH of around 6.5–7.0, the turbid suspension was dialyzed for a whole week against demineralized water. The recovered solution was refrigerated until use, and the weight fraction of CNC concentration in the solution was determined using the gravimetric method.

2.4 Preparing nanocomposite films

The films were produced using a process called solution casting, just like Mohammadi et al., (2020). A predetermined amount of CMC was dissolved in distilled water at 90°C for 30 minutes while being constantly agitated to produce a 100 g solution. Furthermore, gelatin was dissolved in a distinct batch of distilled water at 60 °C with a specified weight (per the design). Then the mixture of CMC and gelatin was heated to 90 °C for 30 minutes while being stirred continuously. The necessary quantity of CNC was dissolved in glycerol (30 wt% of the total solid content of the gelatin and CMC), and the mixture was combined at 90 °C while droplets were added to the CMC/Gelatin solution. The liquid was added to a 130 mm diameter petri dish after 30 minutes of stirring, and air dried for 48 hours to ensure the solvent evaporated gradually. The resultant films were separated from the plate and stored for analysis in a desiccator.

2.5 Analyzing the morphology of nanocomposite films

A scanning electron microscope was utilized to examine the distribution of the CNC fillers in the polymer matrix on a VEGA 3 TESCAN at 5 kV. The film samples were vacuum dried overnight at 40°C and then cryogenically shattered to uncover their cross section for analysis. Before examination, the samples were coated with a 5nm layer of platinum to improve clarity in the scanning electron microscope (SEM).

2.6 Analysis using thermoradimetry

The heat decomposition of cellulose nanocrystals and nanocomposite films was evaluated using an SDT Q600 thermogravimetric analyzer. The samples were cooked in a nitrogen atmosphere from 0°C to 500°C at a rate of 10°C/min for a total of 3.8 mg.

2.7 Determination of WVP

WVP was calculated using the gravimetric method in accordance with ASTM E96/E96M-05 (2005). 4g of anhydrous calcium chloride ($CaCl_2$) was placed in a glass container with the specified diameter and depth in order to achieve a relative humidity (RH) of 0. In a desiccator with potassium sulfate (K_2SO_4) at a temperature and relative humidity of 98%, the glass bottle was covered in the nanocomposite film, weighed, and placed. The sample was measured once every 24 hours in order to determine how the weight of the glass bottle changed over time. Slopes were produced using a linear regression (weight change versus time). The water vapour transfer rate was calculated by dividing the diameter of the plastic bottle opening (m^2) by the gradient of the straight line (g/h) (WVTR). Following that, the WVP (g/(m x h x Pa)) was calculated as stated in the equation below.

$$\text{WVP} = \frac{WVTR}{S(R_1 - R_2)} X \quad (1)$$

where X is the film's thickness in meters, S is the saturated water vapour pressure in pounds at the test temperature of twenty-five degrees Celsius, and R_1 and R_2 are the relative humidity in the climate chamber and the glass bottle, respectively.

2.8 Deterioration of nanocomposite films in soil

The soil degradation test was conducted as described by Salisu et al., (2012) with a few minor adjustments. The test films were weighed and positioned at a depth of 6 cm in a container filled with sand. The samples were carefully taken out of the soil every five days for 40 days in order to determine the weight loss.

III. RESULTS AND DISCUSSION

The CNC arrangement in the CMC-gelatin mixture as observed under an electron microscope scanning is depicted below. In the micrograph of the unstrengthened film, there were a few boundless aggregates and a few abrupt fractures that may have been caused by inadequate smoothness during the film-making operation (Ma et al., 2017). As a result, for films enhanced using five weight percent cellulose nanocrystal, interconnectivity as well as stable nanostructures composed of cellulose

nanocrystal and matrices were observed. However, the CMC-Gelatin film supplemented with 10% cellulose nanocrystals showed some superficial inhomogeneity and substantial splitting. This might be due to increased CNC strengthening, which causes more agglomeration and decreased dispersibility. The compact aggregation of CNCs, as per Kumar et al., (2020), shows that the chains of CNCs display potent hydrophilic contacts with intermolecular hydrogen bonds. In addition, consistent nanostructures made of cellulose nanocrystal and networks were observed for films enhanced using 5 wt% cellulose nanocrystal, with a diameter of approximately of 31 nm for the isolated CNCs and sizes spanning between 20 nm to 50 nm.

The 10 wt% CNC augmented CMC-Gelatin film, however, showed substantial fracturing and some superficial imperfections. It could be due to increased CNC fortification, which causes greater clumping and decreased miscibility. The tight assemblage of CNCs, as per Kumar et al., (2020), shows that the networks of CNCs display potent aqueous contacts and strong hydrogen bonds. The segregated CNCs were found to have sizes spanning between 20 nm to 50 nm, with a mean size of 31 nm. Although this region is similar to that shown by Agustin et al., (2013) utilizing onion shoots (30-50 nm). Zhou et al., (2017) observed ranges around 10 nm as well as 50 nm for CNC synthesized using silk plant, and Benini et al., (2018) documented 10-60 nm with CNC utilizing Imperata brasiliensis vegetation. According to Kargarzadeh et al., (2017), the width of rice husk fiber was lowered by 15-20 nm.

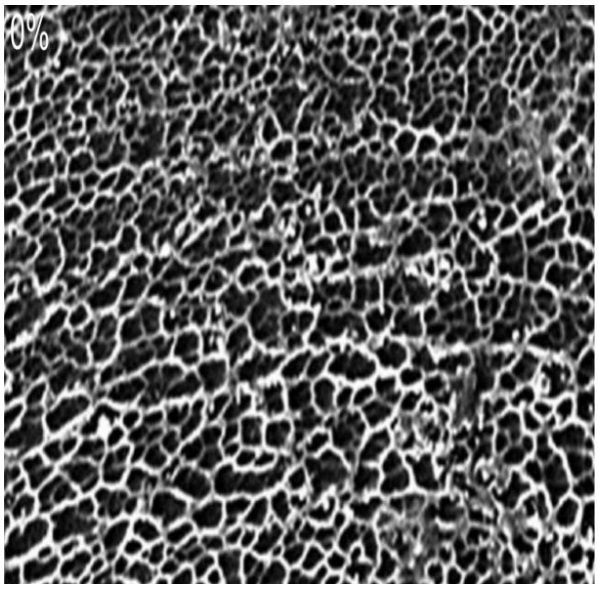

(a) 0% CNC film

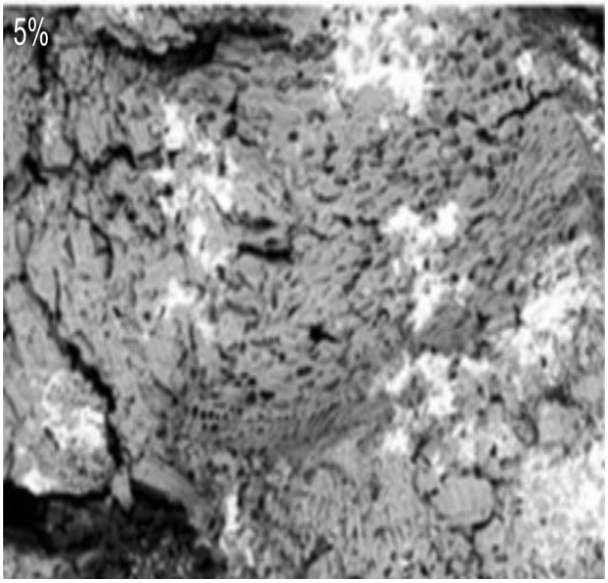

(b) 5% CNC reinforced film

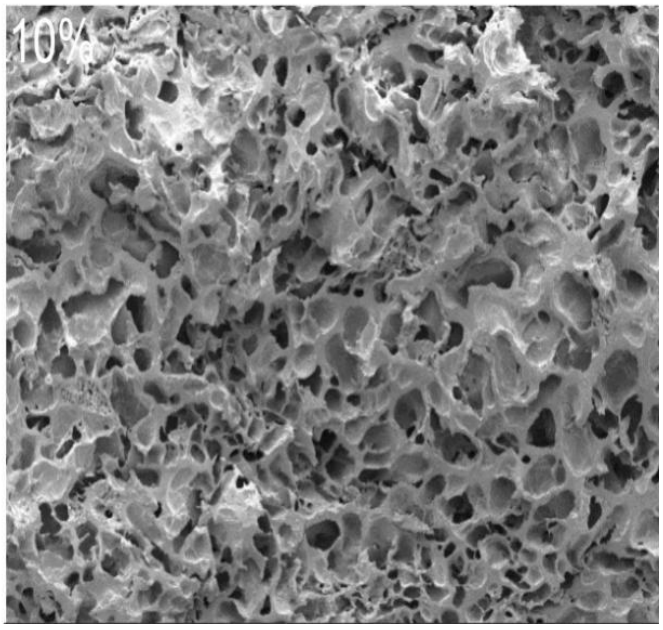

(c) 10% CNC reinforced film

FIGURE 1: Scanning electron micrograph of the nanocomposite films; (i) 0 wt% CNC, (ii) 5 wt% CNC, and (iii) 10 wt% CNC

3.1 Thermal evaluation

Thermogravimetric analysis (TGA) as well as differential thermogravimetric analysis was implemented to investigate the thermal properties of the CNC and nanocomposites (DTG). The results show that below 284°C, the nanocomposites remained thermostable. Because of this, neither CNC nor the nanocomposites was capable of maintaining upwards of 90% of their original weight at this temperature. Its depolymerization, dewatering, as well as disintegration of glycosylation units are assumed to be the main contributors to CNC degradation between 284°C and 286°C. Zhou et al., (2017) found a 245°C beginning decomposition temperature, which really is equivalent to the findings of this study. Early on in the heating process, the weight of the CNC experiment progressively dropped since the sample contained free water (Xu et al., 2017). The CNC's highest temperature of deterioration, as indicated by the DTG curve, was 407°C.

The maximal degrading temperature of 364°C for CNC has indeed been recorded (Benini et al., 2018). The major thermal decomposition threshold for cellulosic materials is typically thought to vary between 200°C and 400°C, and so this optimum degeneration temperature fits in that range (Agustin et al., 2014).

The weight loss was reasonably steady above 400°C and produced a 32% char residue. The sulphate groups formed after sulphuric acid hydrolysis could have had an influence on the amount of residue that was left following the breakdown. The curve patterns with in CMC-gelatin nanocomposite films both with and without reinforcing were similar, however the addition of CNC improved their thermostability. The 5 wt% as well as 10 wt% CNC strengthened films declined at 285°C as well as 286°C, respectively, while the unreinforced film started to deteriorate at 284°C.

According to the DTG graph, the deterioration temperature of such nanocomposite films considerably rose from 390 °C for the unstrengthened film to 400 °C and 407 °C with both the inclusion of 5 wt% as well as 10 wt% CNC, respectively. CNCs showed that they marginally improved the thermostability of the nanocomposite by serving as just an insulation as well as mass transport barrier towards the volatile compounds released upon decomposition (Benini et al., 2018).

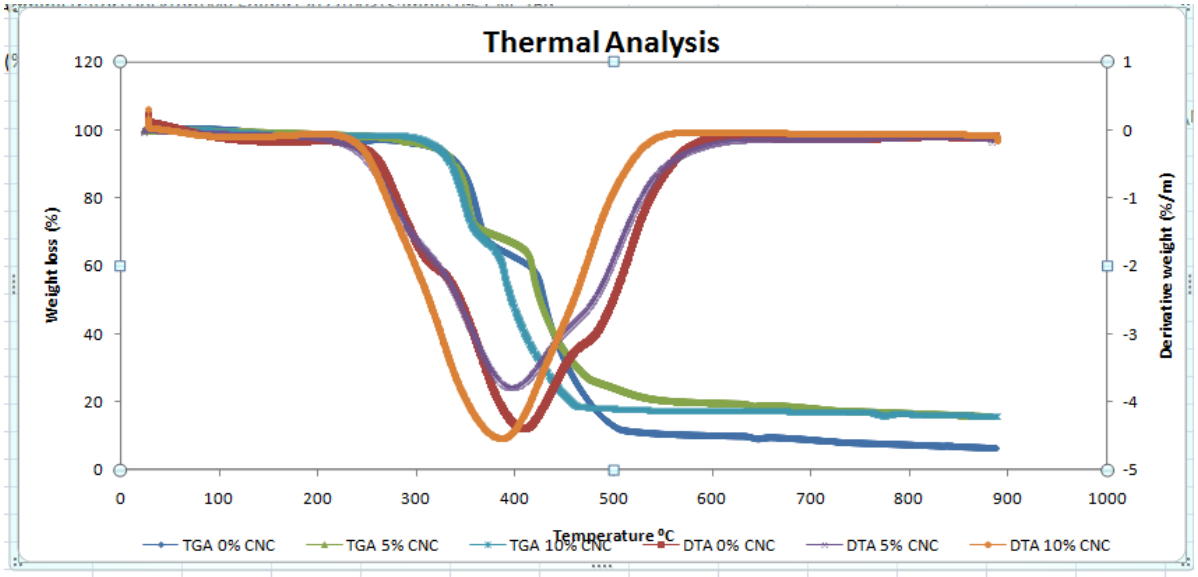

FIGURE 2: Thermal degradation of the nanocomposites

3.2 Water Vapour Permeability

For applications such as packaging, films are expected to at the absolute least lessen gaseous transmission across wrapped items and the environment. This important factor is necessary for avoiding product contamination or packaging-related environmental pollution. The WVP of unstrengthened CMC-gelatin film, 5 wt%, as well as 10 wt% CNC strengthened CMC-gelatin films were examined and reported. The WVP of unstrengthened CMC-gelatin film was calculated to be 2.45 x 10^{-6} g/(m x h x Pa), while for 5 wt% and 10 wt% CNC strengthened films, it was reduced to 1.99 x 10^{-6} g/(m x h x Pa) and 1.73 x 10^{-6} g/(m x h x Pa), respectively.

There is unmistakable proof that the addition of CNC to the CMC-gelatin combination improved the films' WVP. This decrease in WVP can be attributed to the impermeable CNCs, which were evenly dispersed throughout the mix matrix to produce a

circuitous pathway and prolong overall effective diffusion pathway for water vapour transmission (Kanmani and Rhim, 2014; Yadollahi et al., 2014; Bai et al., 2015). The WVP result obtained from this investigation, however, is lower than that reported by Noshirvani et al., since 15% CNC (6.79 x 10^{-7} g/(m x h x Pa)) were introduced to the starch-PVA mixture Noshirvani et al., (2018). Additionally, WVP of 3.7 x 10^{-11} g/(m x h x Pa), which is much lower than the results obtained in this study, was recorded in chitosan/gelatin plasticized using sorbitol as well as glycerol for food containers with a thickness of 0.8 mm (Arvanitoyannis et al., 1998). Similarly, it is assumed that the permeability of a film to water vapor is unrelated to its thickness; yet, hydrophobic films usually exhibit a strong association between their susceptibility and thickness as a result of their attraction to water (Patricia-Miranda et al., 2004). Our research has shown that biodegradable films created by strengthening CMC-gelatin using plantain stem CNC possess excellent WVP for food packaging, in contrast to standard synthetic polymer packaged food films, which are stated to also have WVP in the region of 2.3 x 1014 to 8.7 x 1014 g/(m x h x Pa) (Bastarrachea et al., 2011).

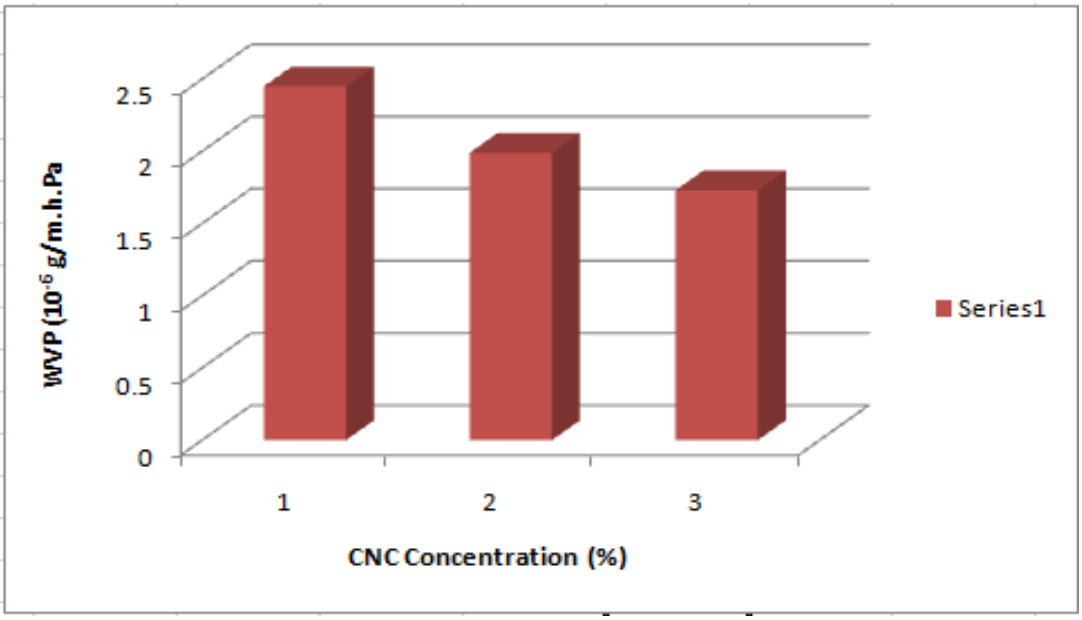

FIGURE 3: Water vapour permeability of the nanocomposite films

3.3 Degrading of the soil

Common polymers including polystyrene, polypropylene, polyethylene terephthalate, and polyethylene are all well recognised for their environmental resistance.

Biodegradability therefore has gained significance when assessing overall environmental impact of polymer in areas such as packaging. The biodegradation behaviors of the 0%, 5%, and 10% CNC strengthened CMC-gelatin films were investigated utilizing the earth immersion strategy. The microbial degradation was studied in regards to the weight loss upon interment in wet soil. The study indicate that the specimen degraded faster compared to the other specimens, despite the fact that significant deterioration wasn't really seen throughout the study period. The degradation of the nanocomposite after first few days of soil burial was essentially similar for both the strengthened and the unreinforced CMC-gelatin films. After 25 days, the unreinforced film showed a higher degree of biodegradability 0.3%, while the 5 wt% as well as 10 wt% CNC strengthened films experienced weight losses of 0.4% as well as 0.5%, correspondingly, attributable to degradability. A superior three-dimensional (3D network) might have resulted from 5 wt% CNC dispersing more evenly in the CMC-gelatin matrix than 10 wt% CNC. Their structural rigidity is readily jeopardized since composites' poor dissemination encourages pressure areas to form in their structure. Although it's crucial to note that equilibrium degradation was not reached in the 35-days timeframe, it's probable that the inclusion of CNC retarded those biodegradation of the films. The strengthened films showed the possibility of continuous deterioration if the disintegration timeframe were protracted, despite the fact that the deterioration rate of the unstrengthened films fell dramatically. After being buried in earth, films quickly disintegrate (Goheen and Wool, 1991; Danjaji et al., 2002); nevertheless, strengthened films have a higher likelihood of ongoing complete breakdown than unstrengthened films, which might also decay gradually beyond 1 month.

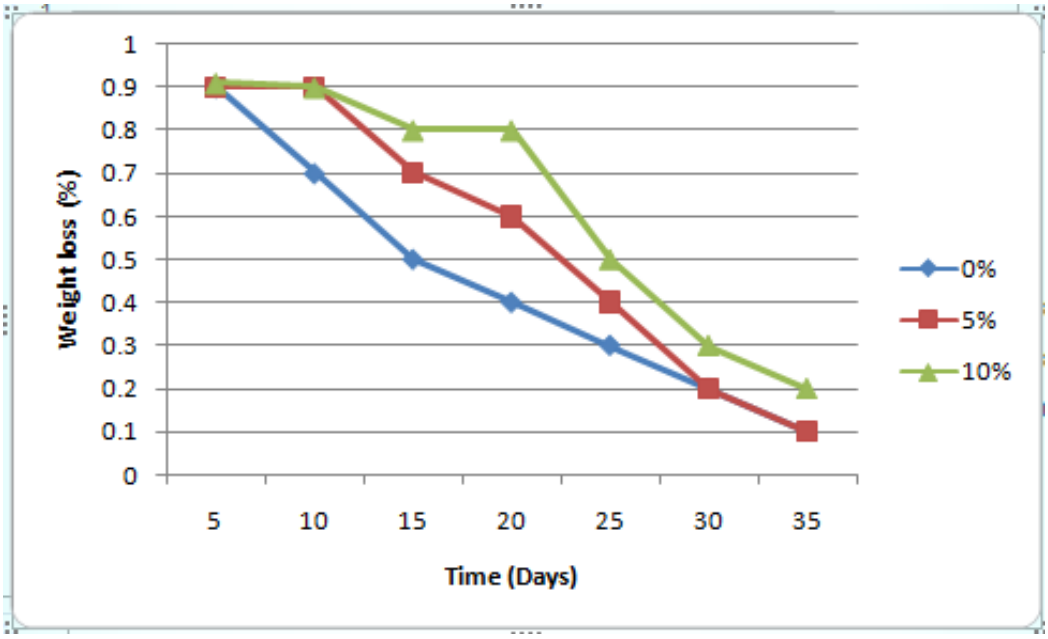

FIGURE 4: Soil burial test of the nanocomposites

IV. CONCLUSIONS

Plantain stem fiber was used to make cellulose nanocrystals with sizes varying from 20 to 50 nm with both the aim of fabricating as well as strengthening nanocomposite films with CMC and gelatin as the matrix for upcoming packaging applications. Interestingly, the thermal efficiency of the CMC-gelatin matrix performed better with the inclusion of CNC. The thermal conductivity of the film was increased to 390–407°C. The enhancement in thermal properties shows that the plantain stem CNC's act as an insulator shielded the volatile compounds released during disintegration from mass transfer. The water vapour permeability of the films under investigation also showed that the inclusion of CNC to the CMC-gelatin matrix decreased the water vapour permeability from 2.45 x 10^{-6} g/(m x h x Pa) to 1.73 x 10^{-6} g/(m x h x Pa). Although hydrophobic, CNC has a higher water barrier property due to its capacity to create a compact three-dimensional framework with the matrix and have less water particle accessibility. The demonstrated findings support the use of plantain stem CNC strengthened CMC-gelatin films as potential sustainable packaging materials, notably for on-the-go food containers.

V. CONFLICT OF INTEREST:

There are no interests in conflict.

AUTHOR CONTRIBUTIONS:

The experiment design was done by E. C. Nwanna; P. C. Eze; L. C. Orakwe; C.P. Nwachukwu; A. E. Ekpo; and J. I. Maduegbuna. The experiment execution was done by E. C. Nwanna; P. C. Eze; C.P. Nwachukwu[1]; and A. E. Ekpo. The data analysis and interpretation was done by E. C. Nwanna; P. C. Eze; L. C. Orakwe and J. I. Maduegbuna. E. C. Nwanna; P. C. Eze; L. C. Orakwe and A. E. Ekpo served as the scientific co-ordinators. All authors reviewed, edited, and approved the manuscript.

REFERENCES

[1] Agustin, M.B., Ahmmad, B., Alonzo, S.M.M., Patriana, F.M., 2014. Bioplastic based on starch and cellulose nanocrystals from rice straw. J. Reinf. Plast. Compos. 33, 2205-2213.

[2] Agustin, M.B., Ahmmad, B., de Leon, E.R.P., Buenaobra, J.L., Salazar, J.R., Hirose, F., 2013. Starch-based biocomposite films reinforced with cellulose nanocrystals from garlic stalks. Polym. Compos. 34, 1325-1332.

[3] Alves, J.S., dos Reis, K.C., Menezes, E.G., Pereira, F.V., Pereira, J., 2015. Effect of cellulose nanocrystals and gelatin in corn starch plasticized films. Carbohydr. Polym. 115, 215-222.

[4] Arvanitoyannis, I.S., Nakayama, A., Aiba, S.I., 1998. Chitosan and gelatin based edible films: state diagrams, mechanical and permeation properties. Carbohydr. Polym. 37, 371-382.

[5] ASTM Standard E96/E96M-05, 2005. Standard Test Method for Water Vapour Transmission of Materials. ASTM International, West Conshohocken, PA Available at www.astm.org/standards.

[6] Bai, H.Y., Sun, Y.L., Xu, J., Dong, W.F., Liu, X.Y., 2015. Rheological and structural characterization of HA/PVA-SbQ composites film-forming solutions and resulting films as affected by UV irradiation time. Carbohydr. Polym. 115, 422-431.

[7] Baiyeri KP, Unadike GO (2001). Ripening stages and days after harvest influenced some biochemical properties of two Nigerian plantains (Musa species AAB) cultivars. Plant prod. Res. J. 6:11-19

[8] Bastarrachea, L., Dhawan, S., Sablani, S.S., 2011. Engineering properties of polymeric-based antimicrobial films for food packaging: a review. Food Eng. Rev. 3, 79-93.

[9] Benini, K.C.C.C., Voorwald, H.J.C., Cioffi, M.O.H., Rezende, M.C., Arantes, V., 2018. Preparation of nanocellulose from *Imperata brasiliensis* grass using Taguchi method. Carbohydr. Polym. 192, 337-346.

[10] Csiszár, E., Nagy, S., 2017. A comparative study on cellulose nanocrystals extracted from bleached cotton and flax and used for casting films with glycerol and sorbitol plasticisers. Carbohydr. Polym. 174, 740-749.

[11] Danjaji, I.D., Nawang, R., Ishiaku, U.S., Ismail, H., Mohd Ishak, Z.A.M., 2002. Degradation studies and moisture uptake of sago-starch-filled linear low-density polyethylene composites. Polym. Test. 21, 75-81.

[12] Edema MO, Sanni LO, Sanni A (2004). Evaluation of plantain flour blends for plantain bread production in Nigeria. Afr. J. Biotechnol. 4 (7): 911-918

[13]El Miri, N., Abdelouahdi, K., Barakat, A., Zahouily, M., Filhri, A., Solhy, A., El Achaby, M., 2015. Bio-nanocomposite films reinforced with cellulose nanocrystals. Rheology of film-forming solutions, transparency, water vapor barrier and tensile propertiesof films. Carbohydr. Polym. 129, 156-167.

[14] Fernández-Braña, Á., Feijoo-Costa, G. & Dias-Ferreira, C. Looking beyond the banning of lightweight bags: analysing the role of plastic (and fuel) impacts in waste collection at a Portuguese city. Environ. Sci. Pollut. Res. 26, 35629–35647 (2019).

[15] Ferreira, F.V., Pinheiro, I.F., Gouveia, R.F., Thim, G.P., Lona, L.M.F., 2017. Functionalized cellulose nanocrystals as reinforcement in biodegradable polymer nanocom-posites. Polym. Compos. 39 E9-E29.

[16] Francisco, W. et al. Functionalization of multi-walled carbon nanotube and mechanical property of epoxy-based nanocomposite. J. Aerosp. Technol. Manag. 7, 289–293 (2015).

[17] Gerritse, J., Leslie, H. A., Caroline, A., Devriese, L. I. & Vethaak, A. D. Fragmentation of plastic objects in a laboratory seawater microcosm. Sci. Rep. 10, 1–16 (2020).

[18] Goheen, S.M., Wool, R.P., 1991. Degradation of polyethylene-starch blends in soil. J. Appl. Polym. Sci. 42, 2691-2701

[19] H. Chi, J. Xue, C. Zhang, H. Chen, L. Li, Y. Qin, Polymers 2018, 10, 1011.

[20] Habibi, Y., Lucia, L.A., Rojas, O.J., 2010. Cellulose nanocrystals: chemistry, self-assembly, and applications. Chem. Rev. 110, 3479-3500.

[21] Han, J.H., Aristippos, G., 2005. Edible films and coatings: a review. Innovations in Food Packaging. Elsevier, Amsterdam, pp. 239-262

[22] Ismaiel, A.M., Salman, H.M.A., Said, H.M., Abd El-sadek, M.S., 2018. Synthesis and characterization of biodegradable polyvinyl alcohol/gelatin polymer blend film based on gamma radiation. Indo Am. J. Pharm. Sci. 5, 3345-3352.

[23] K. Goh, J. K. Heising, Y. Yuan, H. E. Karahan, L. Wei, S. Zhai, J. X. Koh, N. M. Htin, F. Zhang, R. Wang, Acs Appl. Mater. Interfaces 2016, 8, 9994.

[24] Kanmani, P., Rhim, J.W., 2014. Properties and characterization of bionanocomposite films prepared with various biopolymers and ZnO nanoparticles. Carbohydr. Polym. 106, 190-199.

[25] Kargarzadeh, H. et al. Recent developments on nanocellulose reinforced polymer nanocomposites: a review. Polymer 132, 368–393 (2017).

[26] Kargarzadeh, H., Johar, N., Ahmad, I., 2017. Starch biocomposite film reinforced by multiscale rice husk fiber. Compos. Sci. Technol. 151, 147-155.

[27] Ketiku AO, (1973). Chemical composition of unripe green and ripe plantain. J. Sci. Food Agri. 24: 703-707.

[28] Koc, F. E. & Altıncekic, T. G. Investigation of gelatin/chitosan as potential biodegradable polymer films on swelling behavior and methylene blue release kinetics. Polym. Bull. https ://doi.org/10.1007/s0028 9-020-03280 -7 (2020).

[29] Kumar, A., Singh Negi, Y., Choudhary, V., Kant Bhardwaj, N., 2020. Characterization of cellulose nanocrystals produced by acid-hydrolysis from sugarcane bagasse as agro-waste. J. Mater. Phys. Chem. 2, 1-8.

[30] Ma, X.H., Cheng, Y.J., Qin, X.L., Guo, T., Deng, J., Liu, X., 2017. Hydrophilic modification of cellulose nanocrystals improves the physicochemical properties of cassava starch-based nanocomposite films. LWT 86, 318-326.

[31] Mariano, M., Cercená, R., Soldi, V., 2016. Thermal characterization of cellulose nanocrystals isolated from sisal fibers using acid hydrolysis. Ind.Crop. Prod. 94, 454-462.

[32] Mateos-Cárdenas, A., O'Halloran, J., van Pelt, F. N. & Jansen, M. A. Rapid fragmentation of microplastics by the freshwater amphipod Gammarus duebeni (Lillj). Sci. Rep. 10, 1–12 (2020).

[33] Mohammadi M, Azizi MH, Zoghi A. Antimicrobial activity of carboxymethyl cellulose–gelatin film containing Dianthus barbatus essential oil against aflatoxinproducing molds. Food Sci Nutr. 2020;00:1–10. https ://doi. org/10.1002/fsn3.1413

[34] Moon, R. J., Martini, A., Nairn J., Simonsen, J., &Youngblood, J. (2011). Cellulose nanomaterials review: structure, properties and nanocomposites. *Chemical Society Review*, 40(7), 3941–3994.

[35] Mostafa, Y. S. et al. Bioplastic (poly-3-hydroxybutyrate) production by the marine bacterium Pseudodonghicola xiamenensis through date syrup valorization and structural assessment of the biopolymer. Sci. Rep. 10, 1–13 (2020).

[36] Naduparambath, S., Sreejith, M.P., Jinitha, T.V., Shaniba, V., Aparna, K.B., Purushothaman, E., 2018. Development of green composites of poly (vinyl alcohol) reinforced with microcrystalline cellulose derived from sago seed shells. Polym. Compos. 39, 3033-3039.

[37] Nassima El Miri, Karima Abdelouahdi, Abdellatif Barakat, Mohamed Zahouilya, Aziz Fihri, Abderrahim Solhye, Mounir El Achabye, 2015. Bio-nanocomposite films reinforced with cellulose nanocrystals: Rheology of film-forming solutions, transparency, water vapor barrier and tensile properties of films. Carbohydrate Polymers 129 (2015) 156–167

[38] Noshirvani, N., Hong, W., Ghanbarzadeh, B., Fasihi, H., Montazami, R., 2018. Study of cellulose nanocrystal doped starch-polyvinyl alcohol bionanocomposite films. Int. J. Biol. Macromol. 107, 2065-2074.

[39] Ogunola, O. S., Onada, O. A. & Falaye, A. E. Mitigation measures to avert the impacts of plastics and microplastics in the marine environment (a review). Environ. Sci. Pollut. Res. 25, 9293–9310 (2018).

[40] Patricia Miranda, S., Garnica, O., Lara-Sagahon, V., Cárdenas, G., 2004. Water vapor permeability and mechanical properties of chitosan composite films. J. Chil. Chem. Soc. 49, 173-178.

[41] Ramos, M., Jiménez, A., Garrigós, M.C., 2016. Carvacrol-Based Films. Antimicrobial Food Packaging. Elsevier, Amsterdam, pp. 329-338

[42] Salisu, A.A., 2012. Preparation and characterization of biodegradable poly(vinyl alcohol)/starch blends. Chem. Search J. 3, 34-37.

[43] Scaffaro, R., Lopresti, F., D'Arrigo, M., Marino, A. & Nostro, A. Efficacy of poly(lactic acid)/carvacrol electrospun membranes against Staphylococcus aureus and Candida albicans in single and mixed cultures. Appl. Microbiol. Biotechnol. 102, 4171–4181 (2018).

[44] Tang, X.Z., Kumar, P., Alavi, S., Sandeep, K.P., 2012. Recent advances in biopolymers and biopolymer-based nanocomposites for food packaging materials. Crit. Rev. Food Sci. Nutr. 52, 426-442

[45] Thompson, R. et al. New directions in plastic debris. Science 310, 1117–1118 (2005).

[46] Xu, Y.X., Scales, A., Jordan, K., Kim, C., Sismour, E., 2017. Starch nanocomposite films incorporating grape pomace extract and cellulose nanocrystal. J. Appl. Polym. Sci. 134, 44438.

[47] Yadollahi, M., Namazi, H., Barkhordari, S., 2014. Preparation and properties of carboxymethyl cellulose/layered double hydroxide bionanocomposite films. Carbohydr. Polym. 108, 83-90.

[48] Yaradoddi, J. S. et al. Alternative and renewable bio-based and biodegradable plastics. in Handbook of Ecomaterials (eds Martínez, L. et al.) (Springer, Cham, 2019).

[49] Zhou, L., He, H., Jiang, C., Ma, L., Yu, P., 2017. Cellulose nanocrystals from cotton stalk for reinforcement of poly (vinyl alcohol) composites. Cellulose Chem. Technol. 51, 109-119.

Assessment of Probiotic Properties and Consumer Acceptability of Yogurt Made from Commercial Milk using Bacterial Isolates from *NONO*

Oranu M. I[1*], Okonkwo I. F.[2], Onwumelu I. J.[3], Okafor E. C.[4], Ekwealor C. C.[5]

[1,2,5]Department of Applied Microbiology and Brewing, Nnamdi Azikiwe University, Awka
[3]Department of Animal Science & Production, *Dennis* Osadebay *University, Asaba, Delta State, Nigeria*
[4]Department of Animal Science & Technology, Nnamdi Azikiwe University, Awka
*Corresponding Author

Received: 07 September 2023/ Revised: 15 September 2023/ Accepted: 22 September 2023/ Published: 30-09-2023

Abstract— *Nono is a traditionally fermented milk product commonly consumed in parts of Nigeria. It undergoes spontaneous fermentation by lactic acid bacteria (LAB), conferring potential probiotic properties. This study isolated and identified LAB from Nono and assessed their suitability as novel starter cultures for yogurt production using commercial milk. Three LAB isolates were obtained from Nono samples on selective media. They were Gram-positive rods, catalase-negative, with ability to ferment various sugars. The isolate with the greatest antimicrobial activity against Escherichia coli and Staphylococcus aureus was molecularly identified as Lactobacillus fermentum. Set-type yogurt was produced at laboratory scale by inoculating reconstituted commercial milk (14% total solids) with 2% of commercial starter culture (Lactobacillus delbrueckii subsp. bulgaricus and Streptococcus thermophilus); 2% L. fermentum; and 1% each of commercial starter and L. fermentum. The probiotic, physicochemical, sensory and storage properties were analyzed. L. fermentum-containing yogurts had lower pH and higher titratable acidity than the control yogurt. Proximate composition was similar across samples. Sensory evaluation showed comparable consumer acceptability, with slight preference for the control sample. Yogurt with L. fermentum maintained higher viable LAB during storage at refrigeration temperature for 28 days. The findings demonstrate the potential for using LAB isolates from traditionally fermented foods like Nono as novel starter cultures in yogurt manufacture. This can promote product diversification and valorization of indigenous fermentation practices.*

Keywords— Nono, lactic acid bacteria, yogurt, probiotics, starter culture, consumer acceptability.

I. INTRODUCTION

Probiotics are live microbial food supplements that confer health benefits on the host when consumed in adequate amounts (Hill *et al.,* 2014). Fermented foods are regarded as important probiotic carriers, with yogurt being the foremost dairy product acclaimed for its probiotic properties (Granato *et al.,* 2010). Yogurt popularity has surged in recent years due to associated nutritional and therapeutic advantages (Hekmat and Reid, 2006). Its industrial production involves fermentation of milk by starter cultures consisting principally of *Lactobacillus delbrueckii* subsp. *bulgaricus* and *Streptococcus thermophilus* (Sfakianakis and Tzia, 2014). These bacteria impart yogurt's characteristic texture, flavor and acidity by producing lactic acid from lactose fermentation (Gonzalez-Gonzalez *et al.,* 2011).

Besides the traditional yogurt starters, other lactic acid bacteria (LAB) can also be incorporated as adjunct cultures to diversify yogurt products. For instance, *Lactobacillus acidophilus*, *Lactobacillus casei* and *Bifidobacterium* spp. are often used as probiotic enrichments in commercial yogurts to enhance health attributes (Donkor *et al.,* 2007). A growing consumer preference for natural, minimally processed foods has fueled interest in using novel LAB strains isolated from traditional fermented products as starter cultures (Bourdichon *et al.,* 2012). Such strains possess inherent robustness and diverse enzymatic activities tailored by years of adaptation to their natural niches. This can potentially improve yogurt functionality, quality and uniqueness (Leroy and De Vuyst, 2004).

Nono is a traditional fermented milk product widely consumed in Northern Nigeria for its nutritional value. It is produced by Fulani pastoralists through spontaneous fermentation, relying on back-slopping with previous batches to propagate the microbiota (Beukes *et al.,* 2001; Oguntoyinbo and Narbad, 2015). *Nono's* fermentation profile and microbial diversity have been elucidated in a few studies. Isolates obtained include *Lactobacillus delbrueckii, Lactobacillus fermentum, Lactobacillus plantarum, Lactobacillus brevis, Leuconostoc lactis, Leuconostoc mesenteroides* and *Pediococcus acidilactici* (Banwo *et al.,* 2020). *Nono* thus represents a promising reservoir of novel LAB that can be harnessed for functional starter culture development. This study therefore aimed to isolate and identify LAB from *Nono*, evaluate their probiotic properties, and assess the physicochemical qualities, consumer acceptability and stability of yogurt made by incorporating selected *Nono* isolates alongside conventional starter cultures in commercial milk fermentation.

II. MATERIALS AND METHODS

2.1 Sample Collection

Nono samples were purchased from a local producer in Gariki, Amansea, Anambra State, Nigeria and immediately transferred aseptically into sterile flasks. Commercial full cream powdered milk and conventional yogurt starter culture (Yogurmet, France) containing *L. bulgaricus* and *S. thermophilus* lyophilized direct-vat-set cultures were also obtained from Eke Awka Market, Awka, Anambra State, Nigeria.

2.2 Isolation and Identification of LAB from Nono

MRS (de Man, Rogosa and Sharpe) agar (pH 5.4) was used to selectively isolate *Lactobacillus* spp. from the *Nono* samples by anaerobic pour plate technique, while TOS-MUP (transgalactosylated oligosaccharides-mupirocin lithium salt) agar facilitated selective isolation of *Bifidobacterium* spp. based on the methodology described by Süle *et al.* (2014). Discrete colonies were randomly picked and purified by successive subculture on fresh media. Also, Isolates were screened by Gram staining, catalase and oxidase tests. Three presumptive LAB isolates that were Gram-positive rods, catalase-negative and oxidase-negative were selected for further characterization (Süle *et al.*, 2014). Their ability to ferment different sugars was assessed using inverted Durham tubes in peptone water with 1% sugar substrates. The isolate exhibiting greatest antibacterial activity was identified by 16S rDNA sequencing using genomic DNA extraction, PCR amplification with universal primers and Sanger sequencing (Magray *et al.*, 2020). The ~1500 bp 16S rRNA sequence obtained was matched against the NCBI GenBank database using BLASTn to determine closest phylogenetic relatives.

2.3 Preparation of Yogurt Samples

The powdered milk was reconstituted to 14% total solids based on standard methods (Suzanne, 2003) and pasteurized at 90^{o}C for 15 minutes. It was cooled to 42^{o}C and inoculated with different starter cultures as follows:

S - 2% commercial yogurt starter

SP - 2% *Lactobacillus* isolate from Nono

Mix - 1% commercial yogurt starter + 1% *Lactobacillus* isolate

Inoculated milk samples were incubated at 42^{o}C for 4 hours to achieve a titratable acidity of 0.9% lactic acid. The yogurts were then cooled to 4^{o}C and analyzed while fresh (day 0) as well as on days 14 and 28 of refrigeration storage. All experiments were performed in triplicate.

2.4 Assessment of Probiotic Properties of LAB Isolates

2.4.1 Antimicrobial Activity

The agar well-diffusion assay was used to evaluate cell-free supernatants of LAB isolates against *Escherichia coli* ATCC 25922 and *Staphylococcus aureus* ATCC 12600 as described previously (Barefoot and Klaenhammer, 1983). Zones of inhibition were measured after 24h incubation.

2.4.2 Acid Tolerance

Isolates were grown in broth, harvested by centrifugation and resuspended in sterile phosphate buffered saline (pH 7.0) at 10x concentration. This cell suspension was inoculated (1% v/v) into simulated gastric juice (pepsin 3g/L in saline, pH 2.0) and viable counts were determined after 0, 1, 2 and 3h by plating dilutions on MRS agar (Shehata *et al.,* 2016).

2.4.3 Bile Tolerance

Similarly, washed isolate suspensions were inoculated into MRS broth containing 0.3% oxgall bile (HiMedia, India). Viable counts and optical density (625 nm) were monitored after 0, 1, 2 and 3h incubation to assess bile tolerance (Shehata *et al.,* 2016).

2.5 Analysis of Yogurt Quality

2.5.1 pH and Titratable Acidity

Yogurt samples were stirred with distilled water before measuring pH directly using a digital pH meter. Titratable acidity expressed as % lactic acid was determined by titrating yogurt samples with 0.1N NaOH using phenolphthalein indicator (AOAC, 2005; AOAC, 1990).

2.5.2 Viscosity

Viscosity (Pa.s) was measured using a Brookfield viscometer at 150 rpm and 25oC on fresh and stored yogurt samples.

2.5.3 Proximate Analysis

Moisture, fat, protein, ash and carbohydrate content of fresh yogurt samples were analyzed using standard AOAC methods (AOAC, 2005; AOAC, 1990). Total carbohydrate was estimated by difference.

2.5.4 Lactic Acid Content

Lactic acid concentration was determined spectrophotometrically using 0.2% $FeCl_3$ reagent and comparing absorbance at 390 nm against a standard curve of known lactic acid concentrations (Borshchevskaya *et al.,* 2016).

2.5.5 Sensory Evaluation

A 9-point hedonic scale test was conducted with 20 untrained panelists to evaluate the appearance, color, aroma, taste, texture and overall acceptability of fresh yogurt samples. The scales were anchored at 1 for extreme dislike and 9 for extreme like (Udezor, 2012).

2.6 Microbiological Analysis

2.6.1 Antibacterial Activity

Cell-free supernatants were prepared from yogurt samples and their ability to inhibit *Escherichia coli* ATCC 25922 was evaluated by agar well-diffusion assay on days 0, 14 and 28 of refrigeration storage.

2.6.2 Viability of Starter Cultures

Serial dilutions of yogurt samples were plated on MRS agar and incubated anaerobically at 37oC for 48 hours to determine viable LAB counts on days 0, 14 and 28 of storage.

2.7 Data Analysis

All data were analyzed by one-way ANOVA and Duncan's multiple range test using SPSS version 20.0. Mean values were considered significantly different at $p<0.05$.

III. RESULTS

3.1 Isolation and Identification of Probiotic Bacteria

A total of three lactic acid bacteria were isolated from *nono* samples on MRS agar. The isolates were characterized biochemically and identified as rod-shaped, Gram-positive, catalase-negative bacteria resembling Lactobacillus species (Table

1). Further identification of the isolates was done by 16S rDNA sequencing, which revealed isolate B to be *Lactobacillus fermentum* strain 17-6 (Figure 1).

TABLE 1
BIOCHEMICAL CHARACTERIZATION OF LACTIC ACID BACTERIA FROM *NONO*

Biochemical Tests	Isolate A	Isolate B	Isolate C
Gram stain	+	+	+
Cell morphology	Rod	Rod	Rod
Catalase reaction	-	-	-
Oxidase	+	+	+
Glucose fermentation	+	+	+
Gas from glucose	-	-	+
Lactose fermentation	+	+	+
Sucrose fermentation	+	+	+
Galactose fermentation Probable Organism	+ *Lactobacillus* sp.	+ *Lactobacillus* sp..	+ *Lactobacillus* sp.

Keys: (+) = positive test; (-) = negative test; Sp = Species

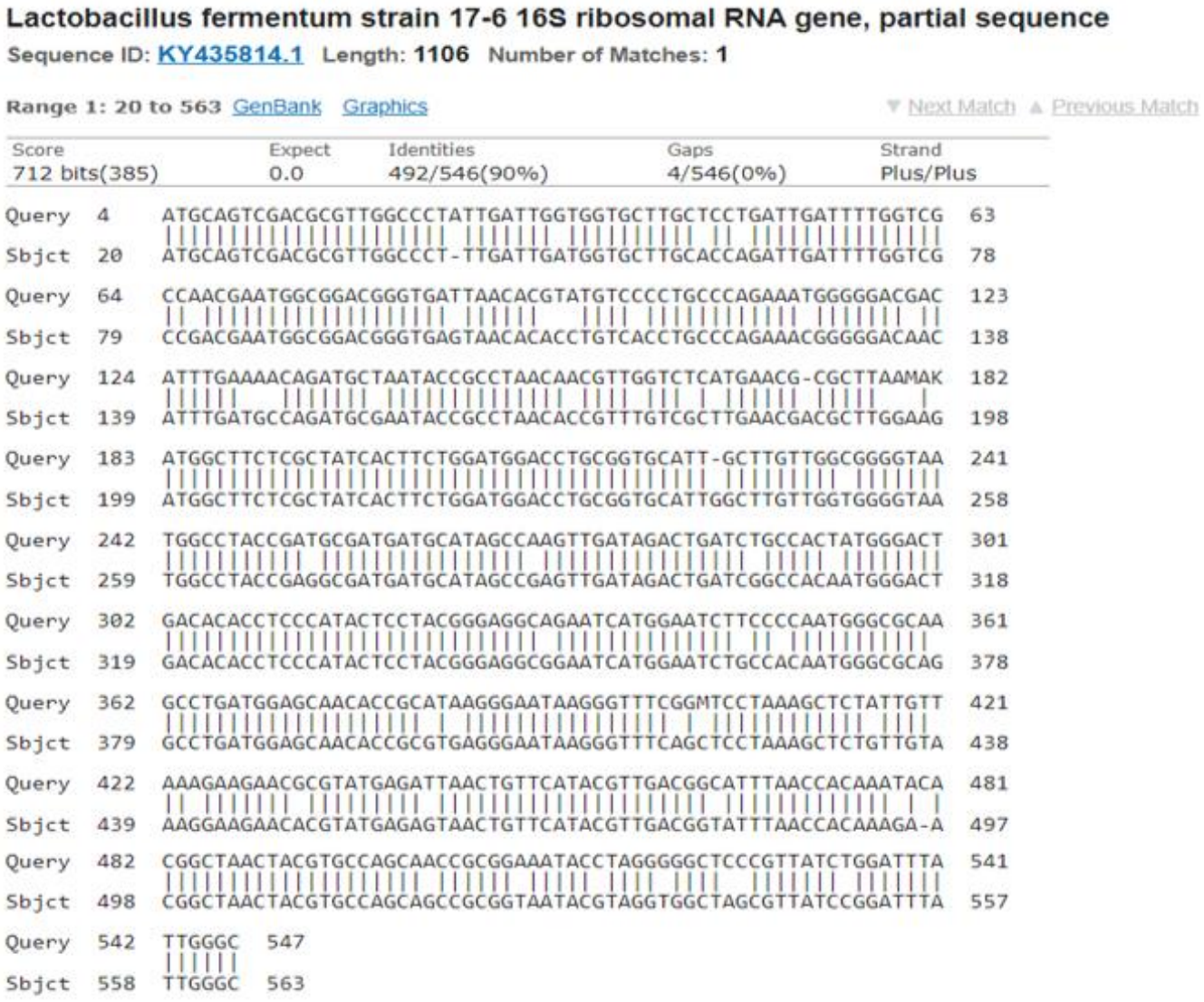

FIGURE 1: Gene Sequence of *Lactobacillus fermentum*

3.2 Assessment of Probiotic Properties

The three isolates were assessed for various probiotic characteristics including acid tolerance, bile tolerance and antimicrobial activity. Growth at different pH showed that all isolates were able to grow at pH 4.0 and pH 7.0, with maximum growth observed at pH 4.0 (Table 2). This indicates the isolates can survive the acidic conditions of the gastrointestinal tract. Additionally, the isolates demonstrated bile tolerance by growing on MRS agar supplemented with 0.3% oxgall bile, confirming their ability to withstand the physiological concentrations of bile salts (Table 3). Of the three isolates, isolate B (*L. fermentum*) exhibited the strongest antimicrobial activity against *E. coli* and *S. aureus*, with inhibition zone diameters of 20.64 ± 0.04mm and 18.50 ± 0.50mm respectively (Table 4). The antibacterial activity suggests the isolate's potential to inhibit pathogens and maintain gut health. Based on the probiotic characteristics demonstrated, isolate B (*L. fermentum*) was selected for further assessment in yogurt production.

TABLE 2
GROWTH OF LACTIC ACID AT DIFFERENT PH

Isolate codes	pH 2.5	pH 4.0	pH 7.0
A	+	++	++
B	++	+++	++
C	+	++	++

Keys: (+) = positive test

TABLE 3
SURVIVAL OF ISOLATES IN FRESH BOVINE BILE

Isolate Codes	Survival in Fresh Bovine Bile
A	+
B	+
C	+

TABLE 4
DIAMETER ZONES OF INHIBITION (mm) FOR ANTIMICROBIAL ACTIVITY OF PROBIOTIC ISOLATES AGAINST SELECTED PATHOGENS

Isolate Codes	*Escherichia coli*	*Staphylococcus aureus*
A	17.38 ± 0.10	16.67 ± 1.15
B	20.64 ± 0.04	18.50 ± 0.50
C	15.27 ± 0.25	12.47 ± 0.41

3.3 Physicochemical Properties of Yogurt

Yogurt was prepared using a commercial starter culture (S), *L. fermentum* isolate (SP) and a mix of both (mix). The physicochemical properties evaluated were pH, titratable acidity, viscosity and total solids (Table 5). Yogurt S had the highest viscosity (10.51 ± 0.01 Pa.s) and total solids (21.70%), while SP and mix had lower pH values (4.11 ± 0.01 and 4.26 ± 0.01 respectively) and higher titratable acidity indicating increased lactic acid production. This was confirmed by lactic acid quantification, where mix had the highest lactic acid concentration within 24hrs (Figure 2).

TABLE 5
PHYSICO-CHEMICAL EVALUATION OF YOGURT SAMPLES

Parameters	S	SP	Mix
Total solid (%)	21.70	18.90	20.08
pH	4.52 ± 0.03	4.11 ± 0.01	4.26 ± 0.01
Titratable Acidity	1.16 ± 0.02	1.10 ± 0.02	1.21 ± 0.02
Viscosity (Pa.s)	10.51 ± 0.01	8.21 ± 0.01	7.21 ± 0.01

Keys: S = Standard yogourmet; Sp = Lactobacillus fermentum; Mix = Mixture of standard yogurmet plus Lactobacillus fermentum

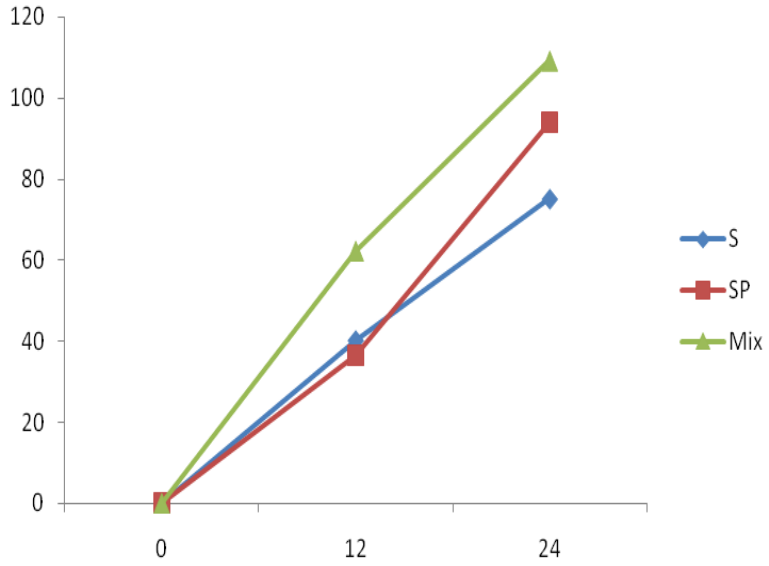

FIGURE 2: Lactic Acid Content of Yogurt Samples
Keys: S- standard yogurmet; SP- Lactobacillus fermentum; Mix- Mixture of standard yogurmet plus lactobacillusfermentum

3.4 Proximate Composition

The nutritional composition of the yogurts was analyzed in terms of moisture, ash, fat, protein, fiber and carbohydrates (Table 6). Yogurt SP had slightly higher moisture, ash, fat and protein compared to S and mix. Notably, SP had higher fiber (3.74%) but lower carbohydrates (5.73%) versus S and mix.

TABLE 6
PROXIMATE COMPOSITION OF YOGURT SAMPLES

Parameters (%)	Sample S	Sample SP	Mix
Moisture content	85	86	84
Ash	0.70	0.80	0.92
Crude fat	3.61	3.74	3.81
Crude protein	3.18	3.2	3.31
Crude fibre	0.51	0.53	0.49
Carbohydrate	7.00	5.73	7.47

Keys: S = Standard yogurmet; Sp = Lactobacillus fermentum; Mix = Mixture of standard yogurmet plus Lactobacillus fermentum

3.5 Sensory Evaluation

Sensory analysis of the yogurts indicated that S had the highest overall acceptability based on appearance, taste and mouthfeel (Table 7). However, there were no marked differences between the samples for aroma and color. This suggests that incorporation of the *L. fermentum* isolate did not adversely affect sensory properties.

TABLE 7
SENSORY EVALUATION OF YOGURT SAMPLES

Parameters	S	SP	Mix
Appearance	8.00	7.00	8.00
Aroma	7.00	7.00	7.00
Taste	8.00	8.50	7.00
Mouth-Feel	6.00	5.00	4.00
Overall Acceptability	8.00	7.00	7.00

Keys: S = Standard yogurmet; Sp = Lactobacillus fermentum; Mix = Mixture of standard yogurmet plus Lactobacillus fermentum

3.6 Storage Viability

The viability of probiotic bacteria and antimicrobial activity against *E. coli* was evaluated during refrigerated storage for 28 days (Tables 8 and 9). Although viable counts decreased over time in all samples, mix maintained the highest counts at day 14 (14.2 x 104 cfu/ml) and day 28 (10.8 x 104 cfu/ml) indicating better probiotic survival. Antimicrobial activity also declined with storage but was likewise highest in mix yogurt compared to S and SP.

TABLE 8
TOTAL VIABLE COUNT (X104) FOR LACTIC ACID BACTERIA FOR THE YOGHURT SAMPLES

Samples	Day 14	Day 28
S	9.2	6.2
SP	10.8	4.5
Mix	14.2	10.8

Keys: S = Standard yogurmet; Sp = Lactobacillus fermentum; Mix = Mixture of standard yogurmet plus Lactobacillus fermentum

IV. DISCUSSION

The present study isolated three lactic acid bacteria from traditionally fermented *Nono* milk, with one isolate identified as *Lactobacillus fermentum* based on 16S rRNA gene sequencing. *Lactobacillus fermentum* has previously been reported as one of the predominant LAB in Nigerian *Nono*, conferring its probiotic properties (Obi *et al.*, 2016). In agreement, our isolated *L. fermentum* strain exhibited good probiotic characteristics including acid and bile tolerance as well as antimicrobial activity against pathogenic *E. coli* and *S. aureus*. These properties enable probiotic bacteria to survive gastrointestinal transit and inhibit pathogens through the production of bacteriocins and organic acids (Granato *et al.*, 2010; Donkor *et al.*, 2007).

Yogurt manufactured by incorporating the *Nono*-derived *L. fermentum* alongside conventional starter cultures demonstrated enhanced physicochemical attributes compared to the control yogurt made solely with starters. Specifically, the *L. fermentum*-containing yogurt had lower pH and higher titratable acidity, indicating increased lactic acid production (Sfakianakis & Tzia, 2014). This was corroborated by direct lactic acid quantification. The higher acidity can extend yogurt's shelf life by suppressing spoilage microorganisms. Despite compositional differences, sensory analysis revealed comparable consumer acceptability across all yogurt samples. This suggests that the *L. fermentum* adjunct did not adversely affect flavor and texture attributes. Mild or no flavor defects upon adding probiotic cultures to yogurt have been documented before (Donkor *et al.*, 2007).

During refrigeration storage, the viability of probiotic bacteria decreased in all yogurts as expected, but viable counts remained significantly higher in the L. fermentum-supplemented yogurt compared to the control after 28 days. Enhanced starter culture survival indicates the robustness of the *Nono* isolate for maintaining yogurt functionality over time (Gonzalez-Gonzalez *et al.*, 2011). In summary, the indigenous *L. fermentum* strain isolated from traditionally fermented *Nono* demonstrated strong

probiotic properties that can be harnessed to develop novel functional starter cultures for yogurt production. Incorporating the isolate improved physicochemical and storage qualities without compromising sensory attributes.

V. CONCLUSION

The findings of this study demonstrate the potential of isolates obtained from traditionally fermented *Nono* to be developed as novel functional starter cultures for yogurt production. The *Lactobacillus fermentum* isolate showed good survival under conditions simulating the gastrointestinal tract, indicating its robust probiotic properties. Incorporation of this isolate into yogurt fermentation enhanced the physicochemical attributes by improving acidification compared to the control. Sensory evaluation revealed comparable consumer acceptability among yogurts produced with different starter combinations. Moreover, viable counts of probiotic bacteria were maintained at a higher level during refrigeration storage of yogurt with added *L. fermentum*. Overall, the results suggest that LAB from indigenous fermented foods like *Nono* have the capacity to be developed as adjunct starter cultures for diverse probiotic dairy products. This offers opportunities to valorize traditional fermentation practices and promote product innovation through strain diversification. Further research could optimize the *Nono* isolate's application in diverse dairy and non-dairy probiotic foods.

REFERENCES

[1] AOAC, 1990. Official methods of analysis 15th edn. Washington D.C. Assoc. of Anal. Chem., pp: 1546

[2] AOAC (2005) Official Methods of Analysis of the Association of Analytical Chemists International. AOAC, Gaithersburg.

[3] Banwo, K., Ogunremi, O. R., & Sanni, A. I. (2020). Fermentation biotechnology of African traditional foods. *Functional foods and biotechnology: Biotransformation and analysis of functional foods and ingredients*, 101-134.

[4] Barefoot, S. F., & Klaenhammer, T. R. (1983). Detection and activity of lactacin B, a bacteriocin produced by Lactobacillus acidophilus. *Applied and Environmental microbiology*, *45*(6), 1808-1815.

[5] Beukes, E. M., Bester, B. H., & Mostert, J. F. (2001). The microbiology of South African traditional fermented milks. *International Journal of Food Microbiology*, *63*(3), 189-197.

[6] Borshchevskaya, L. N., Gordeeva, T. L., Kalinina, A. N., & Sineokii, S. P. (2016). Spectrophotometric determination of lactic acid. *Journal of analytical chemistry*, *71*, 755-758.

[7] Bourdichon, F., Casaregola, S., Farrokh, C., Frisvad, J. C., Gerds, M. L., Hammes, W. P., & Hansen, E. B. (2012). Food fermentations: microorganisms with technological beneficial use. *International journal of food microbiology*, *154*(3), 87-97.

[8] Donkor, O. N., Nilmini, S. L. I., Stolic, P., Vasiljevic, T., & Shah, N. P. (2007). Survival and activity of selected probiotic organisms in set-type yoghurt during cold storage. *International dairy journal*, *17*(6), 657-665.

[9] Gonzalez-Gonzalez, C. R., Tuohy, K. M., & Jauregi, P. (2011). Production of angiotensin-I-converting enzyme (ACE) inhibitory activity in milk fermented with probiotic strains: Effects of calcium, pH and peptides on the ACE-inhibitory activity. *International dairy journal*, *21*(9), 615-622.

[10] Granato D., Branco, G.F., Cruz, A.G., Faria, J.F., and Shah, N.P. (2010). Probiotic dairy products as functional foods.*Comprehensive Reviews in Food Science and Foos Safety*, 9**(5)**, 455-470.

[11] Hekmat, S., and Reid, G. (2006). Sensory properties of probiotic yogurt is comparable to standard yogurt. *Nutrition and Resources*.,26, 163–166.

[12] Hill, C., Guarner, F., Reid, G., Gibson, G. R., Merenstein, D. J., Pot, B., ... & Sanders, M. E. (2014). Expert consensus document: The International Scientific Association for Probiotics and Prebiotics consensus statement on the scope and appropriate use of the term probiotic. *Nature reviews Gastroenterology & hepatology*.

[13] Leroy, F., & De Vuyst, L. (2004). Lactic acid bacteria as functional starter cultures for the food fermentation industry. *Trends in Food Science & Technology*, *15*(2), 67-78.

[14] Magray, A. R., Ganai, B. A., & Ahmad, F. (2020). Isolation, identification and pathogenicity patterns of Mucor hiemalis in cultured Cyprinis carpio communis using challenged system. *Aquaculture*, *518*, 734837.

[15] Obi, C. N., Olugbue, V. U., & Mpamugo, C. P. (2016). Yoghurt production from powdered milk using mixed lactic acid bacteria starter cultures. *Saudi Journal of Pathology and Microbiology*, *1*(2), 42-49.

[16] Oguntoyinbo, F. A., & Narbad, A. (2015). Multifunctional properties of Lactobacillus plantarum strains isolated from fermented cereal foods. *Journal of Functional Foods*, *17*, 621-631.

[17] Udeozor, L.O., 2012. Tiger nut-soymilk drink. Preparation, proximate composition and sensory qualities. Int. J. Food and Nutr. Sci., 1: 18-26.

[18] Sfakianakis, P., & Tzia, C. (2014). Conventional and innovative processing of milk for yogurt manufacture; development of texture and flavor: A review. *Foods*, *3*(1), 176-193.

[19] Shehata, M. G., El Sohaimy, S. A., El-Sahn, M. A., & Youssef, M. M. (2016). Screening of isolated potential probiotic lactic acid bacteria for cholesterol lowering property and bile salt hydrolase activity. *Annals of Agricultural Sciences*, *61*(1), 65-75.

[20] Süle, J., Kõrösi, T., Hucker, A., and Varga, L. (2014).Evaluation of culture media for selective enumeration of bifidobacteria and lactic acid bacteria.*Brazilian Journal of Microbiology*, 45(3), 1023-1030.

[21] Suzanne N (2003). Food Analysis. Purdue University. West lafagette, Indian Plenum pub., pp. 88 -119.

AD Publications
Sector-3, MP Nagar, Bikaner,
Rajasthan, India
www.adpublications.org, info@adpublications.org